

Original Research Article

Effect of calcium phosphate compound (MZF-CaP) with and without fluoride in preventing bone loss in ovariectomized rats

Tomoko Ito^{1,5}, Racquel Z, LeGeros², Manami Takemasa³, Yoshihiro Tokudome^{1,3,6}, Tomohiro Uchino^{1,3,7}, Atsuo Ito⁴, and Makoto Otsuka^{1,3*}

*Corresponding author:

Makoto Otsuka

¹ Research Institute of Pharmaceutical Sciences, Musashino University, Tokyo, Japan

² College of Dentistry, New York University, New York, USA

³ Faculty of Pharmacy, Musashino University, Tokyo, Japan

⁴ National Institute of Advanced Industrial Science and Technology, Ibaraki, Japan

⁵ Present address; Anti-tuberculosis Association, Shinyamanote Hospital, Clinical Medical-Engineering Laboratory, Tokyo, Japan

⁶ Present address; Faculty of Pharmaceutical Sciences, Josai University, Saitama, Japan

⁷ Present address; College of Engineering, Nihon University, Fukushima, Japan

Abstract

Zinc (Zn) has been shown to inhibit osteoclast differentiation, promote osteoblast activity, and enhance the bone formation. Zinc-containing calcium phosphate (Zn-TCP) implanted in rabbit femoral defect was demonstrated to stimulate bone formation. Other studies demonstrated that calcium phosphate compounds (MZF-CaP) incorporating magnesium (Mg^{2+}), zinc and fluoride (F^-) when administered either by injection or orally were effective in preventing bone loss (osteoporosis) induced by estrogen deficiency (ovariectomy) in a rat model. The objective of the present study was to investigate the preventive effect of similar compound, with F (MZF-CaP-L, MZF-CaP-H) and without F (MZ-CaP-L), when injected in ovariectomized (OVX) rats. MZF-CaP-L and MZ-CaP-L were prepared by precipitation at 90°C and MZF-CaP-H was prepared by sintering MZF-CaP-L at 900°C. The release of the ions from acidic buffer was determined. Suspensions of Zn-TCP, MZF-CaP-H, MZF-CaP-L and MZ-CaP-L (617 μg in 0.2 ml of 1% sodium alginate saline solution) were injected intramuscularly under anesthesia into 5-week-old OVX rats on Zn-deficient diet. One week after surgery, bone mineral density (BMD) and bone mineral content (BMC) of the rat femurs were measured using X-ray CT. The injections and X-ray CT and Zn ion plasma measurements were repeated every week for 12 weeks. The rats were sacrificed and the femurs removed after 12 weeks. Bone mechanical strength was evaluated using the three-point bending test. MZ-CaP-L (without F), compared to the other compounds, showed the highest increase in the Zn^{2+} ion plasma concentration, and the highest BMD, BMC and mechanical strength.

Keywords: Calcium phosphate, crystallinity, Osteoporosis, Zinc, Fluorine

Introduction

Osteoporosis results when the rate of bone formation is much lower than the rate of bone resorption resulting in bone loss. It is characterized by thinning and disorganized bone trabecular bone microstructure, leading to bone loss and susceptibility to fractures. Fractures lead to chronic pain, disability, and loss of independence, which decrease in the quality of life [1]. Bone resorption by osteoclasts and formation by osteoblasts are balanced under normal conditions. However, estrogen (female sex hormone) production decreases rapidly in postmenopausal women causing an increase in osteoclastic activity leading to the onset of osteoporosis after menopause [2]. Current osteoporosis therapy includes: calcium (Ca) and vitamin D; vitamin K₂, estrogen, steroids, calcitonin, and bisphosphonates-based drugs [3, 4].

It has been demonstrated that zinc (Zn^{2+}) ions inhibit the differentiation of osteoclasts and promotes osteoblast activity to enhance the formation of hard tissues [3-5]. A clinical relationship between osteoporosis and Zn deficiency has been observed in elderly subjects [6, 7]. Zinc, an essential trace element, is a cofactor of more than 200 enzymes, and is present in nearly every cell type in the body [8]. When a body is deficient in Zn, it induces symptoms such as the facilitation of bone resorption, decreased efficiency of bone formation, skin disease, taste disorders, lowering of the immune system, etc. [9-11].

Zinc-substituted tricalcium phosphate (Zn-TCP) ceramic prepared by Ito et al [12] was demonstrated to stimulate bone formation when implanted in rabbit femora [13]. This stimulatory effect may be attributed to the slow Zn^{2+} ion release from the ceramics.

A calcium phosphate-based material (originally described as MZF-CaP, now also described as synthetic bone mineral, SBM) consisting of apatite incorporating carbonate (CO_3^{2-}), magnesium



(Mg²⁺), fluoride (F⁻) and Zn²⁺ ions was developed by LeGeros [14]. The development of this compound was based on the following rationale: (a) the bone mineral is an apatite incorporating carbonate and magnesium [15] and (b) separately, magnesium, zinc, and fluoride ions, have been associated with biomineralization [6, 8, 9, 16-18]. These experimental compounds (MZP-CaP or SBM) were shown to prevent bone loss induced by estrogen deficiency when administered by injection [19, 20] and prevent bone loss induced by mineral deficiency or estrogen deficiency when administered orally [21-23].

Several ions affect the formation and transformation of biologically relevant calcium phosphates and their incorporation affect the properties of apatites [14, 15]. Incorporation of CO₃²⁻ and/or Mg²⁺ ions increase the crystallinity (crystal size) and decreases the solubility of the apatite [14, 15, 24-28]. On the other hand, incorporation of F⁻ ions increases the crystallinity and decreases the solubility of synthetic or bone apatite [14, 15, 24, 29, 26-28]. Incorporation of Zn²⁺ ions in apatite even though very limited, decreases apatite crystal size and solubility [15, 25]; while Zn substitution in tricalcium phosphate (ZnTCP), stabilizes the structure and decreases its solubility [30].

In this study, formulations with (MZP-CaP-L, MZP-CaP-H) and without (MZ-CaP-L) F were used and their effects in preventing bone loss in ovariectomized rats determined.

Materials and Methods

Materials

Zn-substituted tricalcium phosphate [Ca_{2.7}Zn_{0.3}(PO₄)₂] or Zn-TCP containing 10 mol% Zn (6.17, w/w%) was synthesized as described previously [12]. Apatites incorporating CO₃²⁻, Mg²⁺, Zn²⁺ with (MZP-CaP-L) and without F⁻ (MZ-CaP-L) ions were prepared by hydrolysis method at 90°C [16, 21, 24]. The compositions of the MZP-CaP preparations and Zn-TCP used in this study are summarized in Table 1. MZP-CaP-H was obtained by sintering MZP-CaP-L at 900°C.

Table 1. Composition and specific surface area of apatites.

Samples	Composition (wt %)					Specific surface area (m ² /g)
	Ca	P	Mg	Zn	F	
Zn-TCP	34.1	19.5	-	6.17	-	4.54
MZP-CaP-L	27.2	16.8	1.91	1.83	1.50	55.1
MZ-CaP-L	26.4	17.4	2.00	1.60	0.003	34.4

X-ray diffraction (XRD) analysis

X-ray diffraction (XRD) profiles were obtained with an X-ray diffractometer (RINT-ULTIMA III; Rigaku Co., Japan), using Cu target, Ni filter, operating at 40 kV; current, 40 mA; with scanning speed, 4.0 /min.

Specific surface area measurements

The specific surface area was measured with an MONOSORB (Quantachrome Instruments, USA) by N₂ absorption porosimetry measurements. The powder (about 1g) was loaded into a sample cell and degassed for 1 h at 150 °C prior to analysis. A specific surface area value (m²/g) was measured by a single-point BET method with a MONOSORB.

In vitro release of Zn²⁺ and Ca²⁺ ions from the MZP-CaPs

The release of Ca²⁺ or Zn²⁺ ions from the calcium phosphate samples in acetate buffer solution (pH 5.0) was evaluated. The calcium phosphate powder (10 mg) was added to a stirring acetate buffer solution (100 mL) maintained at 37.0±0.5 °C. An aliquot of 1 mL was sampled every minute and filtered by a membrane filter (0.22 μm). Fresh acetate buffer (1 mL) was refilled to maintain the total volume. Ca²⁺ ion concentration in the filtrate was measured using the methyl xyleneol blue method with a Ca E-Test-Wako (Wako Pure Chemical Industries, Co. Ltd., Tokyo, Japan). Zn²⁺ ion concentration in the filtrate was assessed using the 5-Br PAPS method with a Zn-Test-Wako. Absorbance measurements were performed with a microplate reader (Model 680; BIO-RAD), at 595 nm for Ca, and 550 nm for Zn.

Animal diet

Vitamin D-, Ca- and Zn-deficient diets (DCaZn(-) diet) were obtained from Clea Co. Ltd, Japan. The diet composition is summarized in Table 2.

Table 2. Composition of the diets. Data in the table are from Clea Co. (Japan) and Oriental Yeast Co. (Japan). The DZn(-) diet was prepared by mixing calcium carbonate (1.5%) with the DCaZn(-) diet.

Diet	Vitamin D (IU/100g)	Ca (mg/100g)	Zn (mg/100g)
DCaZn(-)	-	12	0.08
DZn(-)	-	612	0.08
Normal feed	158	1120	5.28

Animal experiments

The animal experiments and maintenance were performed under conditions approved by the animal research committee of Musashino University. Female Sprague-Dawley rats (5 weeks) weighing 160-180 g were anaesthetized by intraperitoneal injection of pentobarbital, and the ovary was extirpated, or treated with sham operation (for healthy rats as positive control). The vitamin D-, Ca- and Zn-deficient diets (DCaZn(-) diet) were fed for a week to prepare the rat osteoporosis model (OVX rat). The rats were assigned randomly into the following 6 groups (8 animals in each group), and treated as follows: Group 1: Healthy rats given with a



sodium alginate saline solution (Normal), Group 2: OVX rats given with a sodium alginate saline solution (Control), Group 3: OVX rats given with Zn-TCP suspension, Group 4: OVX rats given with MZF-CaP-H, Group 5: OVX rats given with MZF-CaP-L, Group 6: OVX rats given with MZ-CaP-L. Each sample containing 617 μg of Zn in 0.2 mL of 1% sodium alginate saline solution was injected intramuscularly under anesthesia into the OVX rats. One week after surgery, bone mineral density (BMD) and bone mineral content (BMC) of the femur of the rats were measured using X-ray CT (pixel size, 480 480 fan beam; tube voltage, 50 kV; tube current, 1 mA; resolution, 0.25 mm) (LCT-100A; ALOKA, Tokyo, Japan). The Rats were kept fed with DZn (-) diet (including CaCO_3) for up to 12 weeks. The injection and X-ray CT measurement were repeated every week, and the concentration of Zn ions in the plasma was also measured. After 12 weeks, the rats were sacrificed, and the femurs were removed. Their bone mechanical strength was evaluated by the three-point bending test with a compression and tensile testing machine (TG-50kN; Minebea Co. Ltd, Japan).

Statistical test

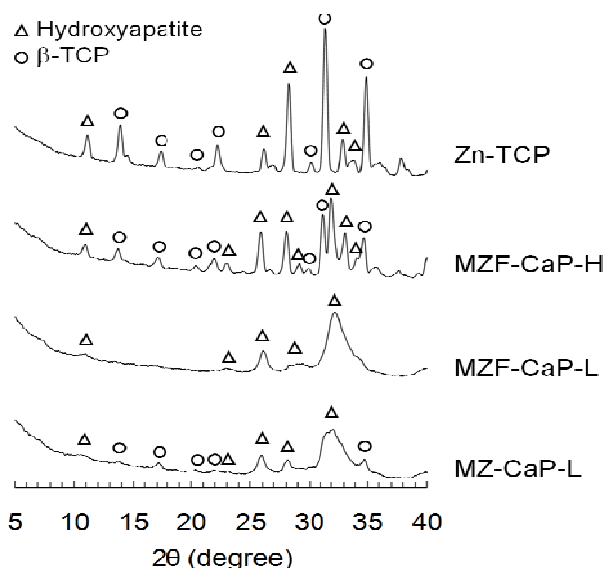
Significant differences between two independent groups were examined using Student's *t*-test. One-way analysis of variance (ANOVA) was used to determine significant differences among six groups.

Results

Characterization of Zn-TCP and MZF-CaPs

X-ray powder diffraction profiles of the test materials (Zn-TCP, MZF-CaP-L, MZF-CaP-H, MZ-CaP-L) are shown in Figure 1.

Figure 1. X-ray powder diffraction profiles of Zn-TCP and MZF-CaPs.



Zn-TCP and MZF-CaP-H, synthesized by sintering, showed sharp diffraction peaks, indicating the high crystallinity of the formulations. The diffraction peaks at $2\theta = 14, 17, 20.5, 22, 30, 31.5$ and 35 degrees two theta ($^{\circ}2\theta$) are attributed to the β -TCP structure. In the structure of MZF-CaP-H (obtained by sintering MZF-CaP-L at 900°C), typical diffraction peaks of hydroxyapatite at $32^{\circ}2\theta$ were detected. On the other hand, MZF-CaP-L and MZ-CaP-L, which were prepared by hydrolysis at 95°C , showed broad apatite diffraction peaks at 26 to $32^{\circ}2\theta$. The broad peaks indicate apatite with low crystallinity (i.e., small crystallite size) (Klug *et al.*, 1974). The XRD profile of MZ-CaP-L showed small diffraction peaks of β -TCP at $14, 17, 20.5, 22,$ and $35^{\circ}2\theta$ in addition to the broad apatite diffraction peaks. The β -TCP is presumably Mg- and Zn-substituted [15].

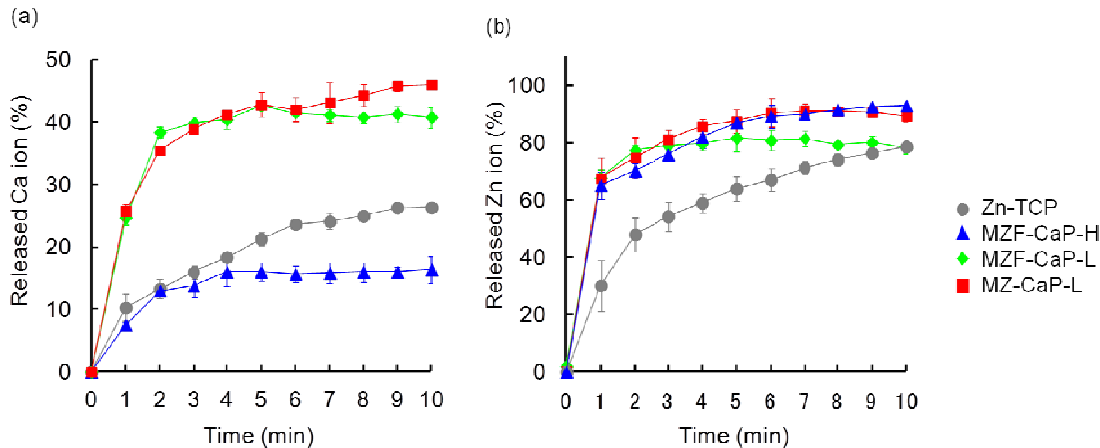
The specific surface areas of Zn-TCP and MZF-CaPs powders were evaluated by the BET nitrogen absorption method. The specific surface area of high-crystalline Zn-TCP and MZF-CaP-H was smaller than that of low-crystalline MZF-CaP-L and MZ-CaP-L (Table 1).

Release of Ca^{2+} and Zn^{2+} ions from MZF-CaPs at pH 5.0

The release profile of Ca^{2+} and Zn^{2+} ions from Zn-TCP and MZF-CaPs powders was examined in acetate buffer (pH 5.0, 37°C). The concentration of the Ca^{2+} ions released from MZF-CaP-L and MZ-CaP-L which had low crystallinity (i.e., small crystallite size) compared to that released from highly crystalline (i.e., large crystallite size) Zn-TCP and MZF-CaP-H. The concentration of the Ca^{2+} ions released from MZF-CaP-H and MZF-CaP-L which contained F ions reached a plateau after about 4 min in the buffer (Figure. 2 (a)).

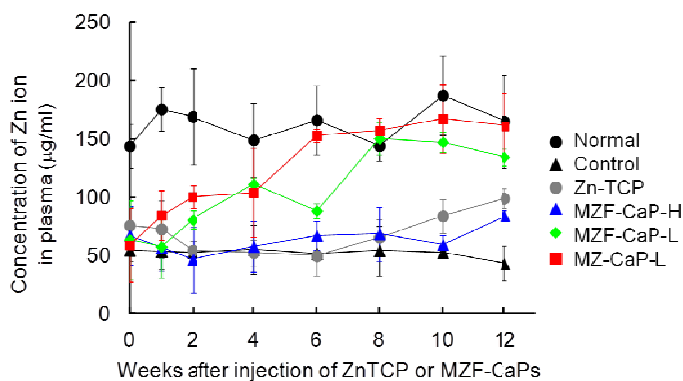
The MZF-CaP-H, MZF-CaP-L and MZ-CaP-L compounds contained Mg. These compounds showed fast initial release of Zn^{2+} ions in the acetate buffer (Figure. 2 (b)). On the other hand, Zn-TCP showed relatively slow release of the ion, and the Zn concentration in the buffer kept increasing for more than 10 min (Figure. 2 (b)).

MZF-CaP-H was synthesized by sintering of MZF-CaP-L and has a crystalline hydroxyapatite structure. F incorporation in the apatite also contributed to the low solubility [15]. However the sintering process caused formation of HA with some β -TCP which has a higher solubility than HA. Therefore the solubility of the MZF-CaP-H is decreased by the incorporation of F in the HA but decreased by the presence β -TCP.

Figure 2. Release profile of (a); Ca ion, and (b); Zn ion from Zn-TCP and MZF-CaPs powders in acetate buffer (pH 5.0) at 37 C.

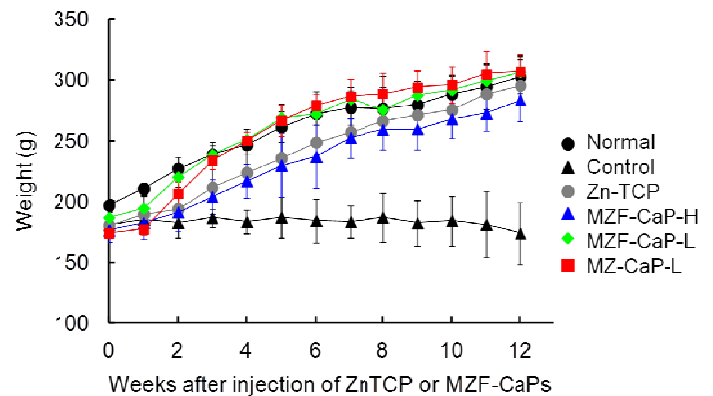
Zn²⁺ ion concentration in plasma

The effect of Zn-TCP or MZF-CaPs on the Zn²⁺ ion concentration in the OVX rat plasma is illustrated in Figure 3. The Zn²⁺ ion concentration in the plasma of rats injected with low-crystalline MZF-CaP-L or MZ-CaP-L increased soon after the injection, and became almost equivalent to that in normal rats after 8 weeks. The relatively slower release of Zn ions was observed with Zn-TCP (which also showed the slow release of ions *in vitro*), and the concentration of Zn²⁺ ions in the plasma rose after 6 weeks.

Figure 3. Concentration of Zn ions in plasma of rats after intramuscular administration of Zn-TCP or MZF-CaPs.

Rat body weight

The body weight of OVX rats injected with Zn-TCP or MZF-CaPs apparently increased compared with non-treated OVX rats (control group) (Figure 4). Notably, MZF-CaP-L or MZ-CaP-L showed the same increase rate of the body weight as the normal group (healthy rats) after the 4th week of injection. The decreasing order of the body weight after 12 weeks was MZ-CaP-L > MZF-CaP-L > Normal > Zn-TCP > MZF-CaP-H > Control.

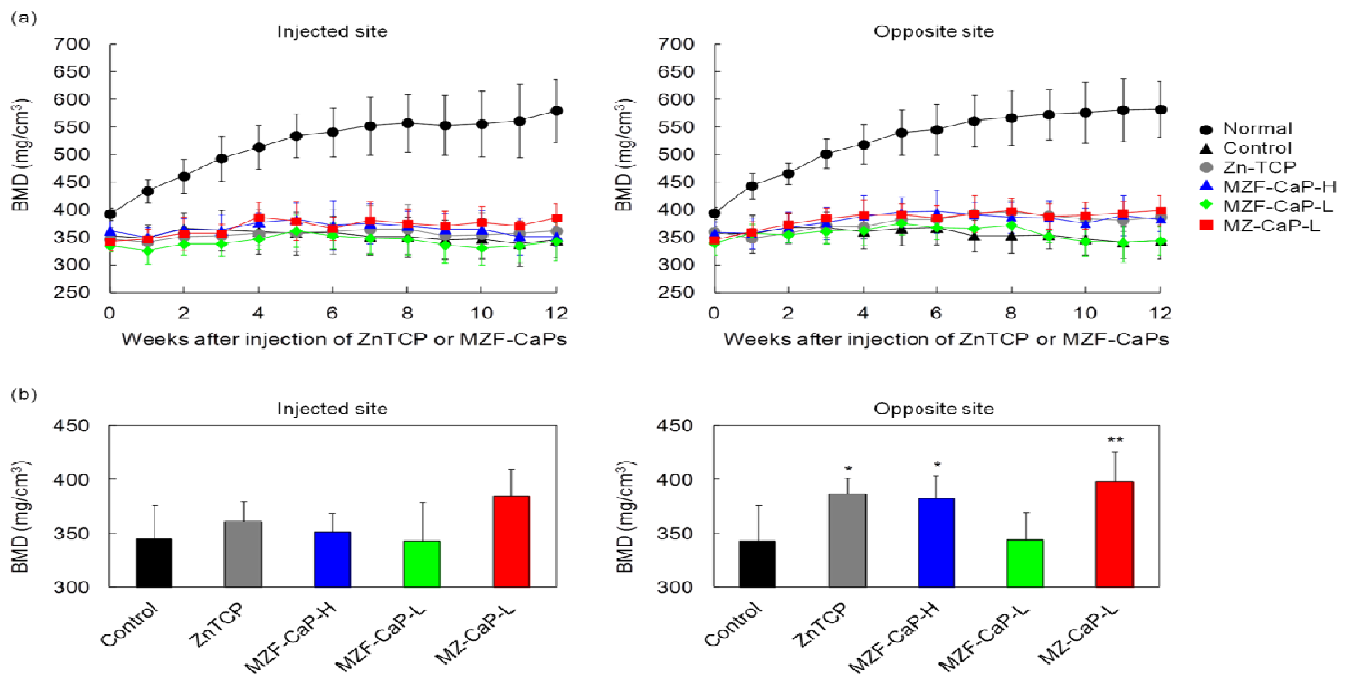
Figure 4. Body weight changes of rats after intramuscular administration of Zn-TCP or MZF-CaPs.

Bone mineral density (BMD) and bone mineral contents (BMC)

The suspension of Zn-TCP or MZF-CaPs was injected intramuscularly into the right femur of OVX rats. The BMD and BMC of right and left femurs were measured by X-ray CT. Unlike normal rats, BMD increase was not observed in OVX rats (Figure. 5a); however, MZ-CaP-L induced a higher BMD value on both sides compared to that in control rats after 12 weeks (Figure. 5b). On the other hand, the BMC of all rats treated with MZF-CaPs improved in both right and left femurs (Fig. 6a). The difference between the control group and treated rats became evident three weeks after the first injection, and the difference from control rats became significant after 6 weeks (Figure. 6b).

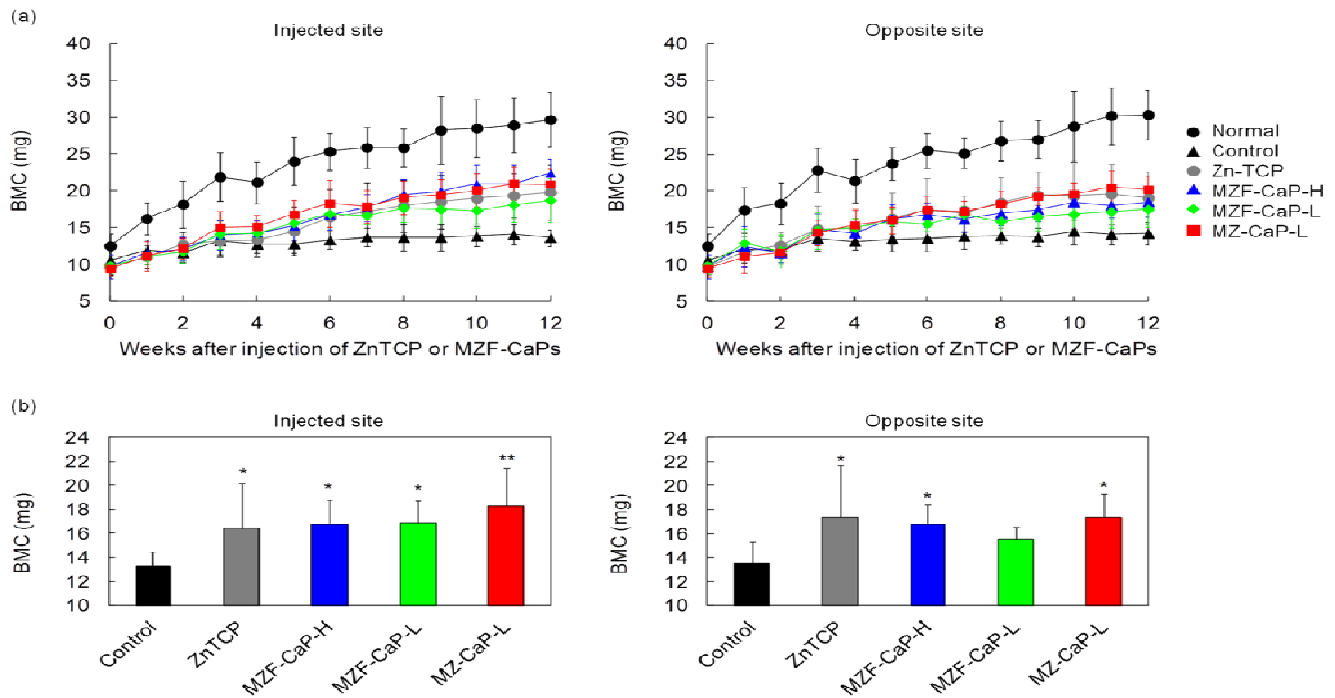


Figure 5. (a) BMD changes in the injected femur and the other side after intramuscular administration of Zn-TCP or MZF-CaPs, and (b) BMD value after 12 weeks.



*: $p < 0.05$, **: $p < 0.01$ vs control

Figure 6. (a) BMC changes of the femurs of rats after intramuscular administration of Zn-TCP or MZF-CaPs, and (b) BMC value after 6 weeks.



*: $p < 0.05$, **: $p < 0.01$ vs control

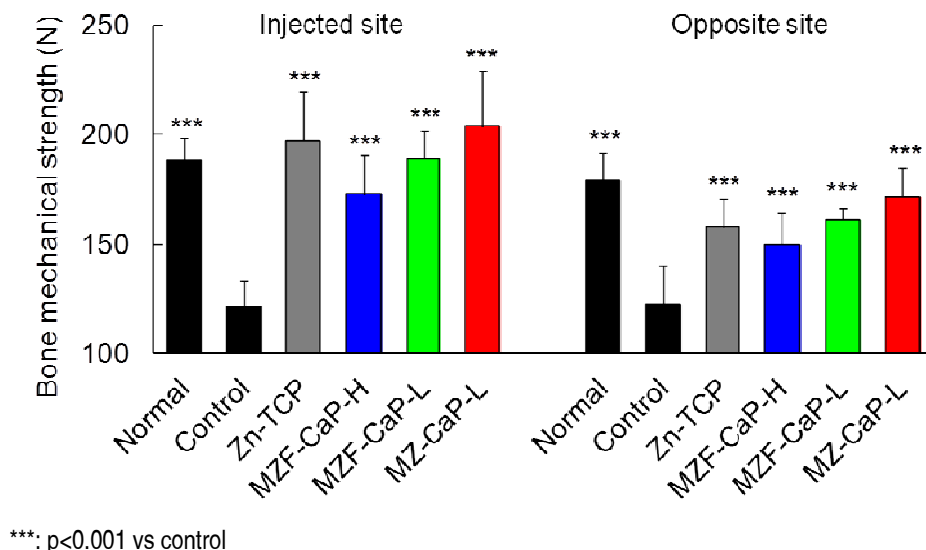


Bone mechanical strength

The bone mechanical strength of both femurs in OVX rats which received injection of Zn-TCP or MZF-CaP suspension is shown in Figure 7. The bone mechanical strength of right and left femurs of healthy normal rats was 188 and 179 N, while that for control OVX rats was 121 and 123 N, respectively, showing that the bone

mechanical strength of all treated rats was significantly higher than the control group. Bone mechanical strength was especially improved in the right femur (the injection site), and OVX rats injected with a low-crystalline MZ-CaP-L (without F), showed the highest bone mechanical strength.

Figure 7. Femur mechanical strength after 12 weeks.



Discussion

The solubility of apatites strongly depend on the crystallinity (crystallite size) and the type and amount of substituting ions [16, 24-26, 28]. For example, increasing carbonate substitution in the apatite causes a decrease in crystallinity (smaller crystallite size) and an increase in solubility while F substitution causes an increase in crystallinity and a decrease in solubility. MZF-CaP-L and MZ-CaP-L, prepared by wet synthesis at low temperature, had low crystallinity. The Ca^{2+} ions were quickly released from these apatites in acetate buffer (pH 5.0, 37°C) owing to the easy dissolution of low-crystalline hydroxyapatite reflected in their higher surface area compared to the highly crystalline Zn-TCP and MZF-CaP-H. On the other hand, the release of the Ca^{2+} ions in the F-containing compounds (MZF-CaP-L and MZF-CaP-H) reached a plateau after about 2 min in the buffer. This may be attributed to the fact that the F-for-OH substitution in the apatite causes the apatite structure to be more stable and less soluble [16]. The release behavior of Zn ion also depended on the components, and MZF-CaP-H, MZF-CaP-L, and MZ-CaP-L including magnesium, showed an initial burst in the release of Zn^{2+} ion release in the acetate buffer. The incorporation of Mg in apatite reduces its crystallinity and increases its solubility [16, 26]. Deformation of the crystalline lattice of hydroxyapatite would easily take place in MZF-

CaP-H, MZF-CaP-L, MZ-CaP-L, and cause the quick release of the zinc ions

Injection of MZF-CaP-L or MZ-CaP-L with high solubility successfully increased the Zn^{2+} ion concentration in the plasma of the OVX rats, up to the same level as normal rats (healthy rats) 8 weeks after the first injection. On the other hand, release of Zn ion from MZF-CaP-H in vivo should be slow because of the limited solubility of such a highly crystalline material, though that in acetate buffer was fairly rapid. In the Zn-TCP-administrated rats, enhancement of the Zn^{2+} ion concentration in plasma was observed 6 weeks after the injection. However, in prior studies [19, 20], increase in the Zn ion concentration was observed at 1 or 2 weeks post-injection. This difference may be attributed to the lower zinc concentration in the Zn-TCP used in the present study (this study: ca. 3.3 mg/kg; prior studies: ca. 3.9 mg/kg [19], ca. 4.9 mg/kg and ca. 4.0 mg/kg [20]) and to the difference in the age of rats.

Body weight increase, a barometer of a healthy condition, in all treated OVX rats was the same rate as healthy rats. The highest bone mineral density and highest bone mechanical strength were observed in the OVX rats injected with MZ-CaP-L which was a low-crystalline apatite, highest solubility. And did not contain F ions. The MZ-CaP-L compound also showed an initial burst of ion release followed by a steady state of slow release. This seemed to

induce a relatively higher zinc concentration in the plasma, causing a whole body effect and improvement in the legs on both sides.

Conclusion

MZ-CaP-L (without fluoride ions), a low-crystalline apatite with the highest solubility, induced high zinc concentration in plasma, causing a whole-body therapeutic effect on OVX rats, such as bone mineral density, bone mechanical strength, and body weight. Application of the system for the treatment of osteoporosis is expected.

References

- [1]. Melton LJ III. Adverse outcomes of osteoporotic fractures in the general population. *J bone Miner Res* 2003; 18: 1139–1141.
- [2]. Rodan GA, Raisz LG, Milezikian JP. Pathophysiology of Osteoporosis. In: Bilezikian JP, Raisz LG, Rodan GA (eds). *Principles of Bone Biology*. Acad Press, New York. 1996; 979–992.
- [3]. Fleisch H, Reszka A, Rodan GA, Rogers M. Bisphosphonates: Mechanisms of Action. In: Bilezikian JP, Raisz LG, Rodan GA (eds). *Principles of Bone Biology* (2nd ed). Academic Press; New York. 2002; 1361–1386.
- [4]. Mauck KF, Clarke BL. Diagnosis screening, prevention and treatment of osteoporosis. *Mayo Clin Proc.* 2005; 81: 662–672.
- [5]. Kishi S, Yamaguchi M. Inhibitory effect of zinc compounds on osteoblast-like cell formation in mouse marrow cultures. *Biochem Pharmacol.* 1994; 48: 1225–1230.
- [6]. Yamaguchi M, Inamoto K, Suketa Y. Effect of essential trace metals on bone metabolism in weanling rats: Comparison with zinc and other metals' actions. *Res Exp Med.* 1986; 186: 337–342.
- [7]. Szathmari M, Steczek K, Szucs J, Hollo I. Zinc excretion in osteoporotic women. *Orv Hetil.* 1993; 134: 911–914.
- [8]. Relea P, Revilla M, Pipoll E, Arribas I, Villa LF, Rico H. Zinc, biochemical markers of nutrition, and type I osteoporosis. *Age Aging.* 1995; 24: 303–307.
- [9]. Williams RJ. Zinc: What is its role in biology? *Endeavour.* 1984; 8: 65–70.
- [10]. Oner G, Bhaumick B, Bala RM. Effect of Zinc Deficiency on Serum Somatomedin Levels and Skeletal Growth in Young Rats, *Endocrinology.* 1984; 114: 1860–1863.
- [11]. Shankar AH, Prasad AS. Zinc and immune function: the biological basis of altered resistance to infection. *AM J Clin Nutr.* 1998; 68: 447S–463S.
- [12]. Ito A, Naito H, Ichinose N, Tateish T. Preparation, solubility, and cytocompatibility of zinc-releasing calcium phosphate ceramics. *J Biomed Mater Res.* 2000; 50: 178–183.
- [13]. Kawamura H, Ito A, Miyakawa S, Layrolle P, Ojima K, Naito H, et al. Stimulatory effect of zinc on bone formation around zinc-releasing calcium phosphate ceramics implanted rabbits femora. *J Biomed Mater Res.* 2000; 50: 184–190.
- [14]. LeGeros RZ. NIBIB/NIH grant number EB 003070. 2007.
- [15]. LeGeros RZ. Apatites in Biological Systems. *Prog. Crystal Growth Charact.* 1981; 4: 1–45.
- [16]. LeGeros RZ. Calcium phosphates in oral biology and medicine. In: Myers HM, editor: *Monogr Oral Sci*. Basel: Karger. 1991; 82–107.
- [17]. Wallach S. Effect of magnesium in skeletal metabolism. *Trace Elem.* 1990; 9: 1–14.
- [18]. Kleerelopper M. Fluoride and the skeleton. In: Bilezikian JP, Raisz LG, Rodan GA, editors. *Principles of bone biology*. Chapter 75. San Diego: Academic Press. 1996; 1053–1062.
- [19]. Otsuka M, Oshinbe A, LeGeros RZ, Tokudome Y, Ito A, Otsuka K, Higuchi WI. Efficacy of a new injectable calcium phosphate ceramic suspension on improving bone properties of ovariectomized rats. *J Pharm Sci.* 2008; 97: 421–432.
- [20]. Tokudome Y, Otsuka M, Ito A, LeGeros RZ. Long-term therapeutic effect of novel calcium phosphate based compounds injected in ovariectomized rats. *J Biomed Mater Res.* 2009; 90B: 2229–237.
- [21]. LeGeros RZ, Mijares D, Yao F, Tannous S, Catig G, Xi Q, Dias R, LeGeros JP. Synthetic bone mineral (SBM) for osteoporosis therapy: Part I. Prevention of bone loss from mineral deficiency. *Key Engineer Mater.* 2008; 361-363: 43–46. Trans Tech Pub, Switzerland.
- [22]. Mijares D. Prevention of bone loss in ovariectomized rat model: Effect of synthetic bone mineral (SBM). MS Thesis. New York University. 2010.
- [23]. Mijares D, Kulkarni A, Lewis K, Yao F, Xi Q, Tannous S, Dias R, LeGeros RZ. Oral bone loss induced by mineral deficiency in a rat model: Effect of a synthetic bone mineral (SBM) preparation. *Arch Oral Biol.* 2012; 57: 1264–1273.
- [24]. LeGeros RZ, LeGeros JP, Trautz OR, Shirra WP. Conversion of monetite, CaHPO₄, to apatites: effect of carbonate on the crystallinity and the morphology

Acknowledgements

This study was supported in part by a grant from the NIBIB/NIH, NIAMS/NIH (#EB003070 and #AR056208, respectively, PI: R. Z. LeGeros) and MEXT; HAITEKU (PI: M Otsuka) from the Ministry of Education, Culture, Sports, Sciences and Technology, Japan.



- of the apatite crystallites. *Adv X-ray Anal* 1971; 14: 57–66.
- [25]. LeGeros RZ, Bleiwas CB, Retino M, Rohanizadeh R, LeGeros JP. Zinc effect on the in vitro formation of calcium phosphates: relevance to clinical inhibition of calculus formation. *Am J Dent*. 1999; 12: 65–70.
- [26]. LeGeros RZ, Sakae T, Bautista C, Retino M, LeGeros JP. Magnesium and carbonate in enamel and synthetic apatites. *Adv Dent Res*. 1996; 10: 225–231.
- [27]. LeGeros RZ, Singer L, Ophaug RH, Quirolgico G, Thein A, LeGeros JP. The effect of fluoride on the stability of synthetic and biological (bone mineral) apatites. In Menzcel J, Robin GC, Makin M, Steinberg R (eds.), *Osteoporosis*, J. Wiley & Sons, New York: 1982; 327–341.
- [28]. LeGeros RZ, Tung MS. Chemical stability of carbonate and fluoride containing apatites. *Caries Res*. 1983; 17: 419–429.
- [29]. Baig AA, Fox JL, Young RA, Wang Z, Hsu J, Higuchi WI, et al. Relationships among carbonated apatite solubility, crystallite size, and microstrain parameters. *Calcif Tissue Int*. 1999; 64: 437–49.
- [30]. Ito A, LeGeros RZ. Magnesium- and Zinc-substituted beta-Tricalcium Phosphate Materials. In: *Progress in Bioceramics*, Vallet-Regi M (Ed). *Key Engineer Mater*. 2008; 377: 85–98. Trans Tech Publications, Zurich.

